Contribution from the Chemistry Department, Faculty of Science,
Australian National University, Canberra, 2600, Australia

Electrochemical and ESR Studies of Molybdenum–Sulfur Donor Complexes. One-Electron Reduction of *cis*-Bis(*N*,*N*-dialkyldithiocarbamato)dinitrosylmolybdenum and -tungsten Complexes

JOHN R. BUDGE, JOHN A. BROOMHEAD,* and PETER D. W. BOYD

Received February 4, 1981

cis-$M(R_2dtc)_2(NO)_2$ complexes (M = Mo or W, R = Me, Et, *i*-Pr, *n*-Bu, Bzl, pyr) undergo a reversible one-electron reduction to give the radical anion $M(R_2dtc)_2(NO)_2^-$. ESR studies have shown that the unpaired electron is delocalized over both nitrosyl groups. No metal hyperfine couplings were observed. Analysis of frozen-solution ESR spectra of $Mo(Et_2dtc)_2(^{15}NO)_2^-$ and $[Mo(Et_2dtc)_2(NO)_2]^-$ has yielded anisotropic **g** and nitrogen hyperfine tensors for these complexes. In addition, the angle between the NO vectors remains essentially unchanged upon reduction of $Mo(Et_2dtc)_2(NO)_2$. These observations strongly support the molecular orbital description of $M(R_2dtc)_2(NO)_2^-$. Here, the unpaired electron resides in a dinitrosyl-based molecular orbital which possesses virtually no metal d-orbital character and which is close to nonbonding between the two NO groups.

Introduction

Recently, ^{15}N-labeling and kinetic studies[1] were reported for the complicated nitrosyl reaction that occurs when *cis*-$Mo(R_2dtc)_2(NO)_2$ complexes (R_2 = Me_2, *i*-Pr_2, *n*-Br_2, Bzl_2, and pyr)[2] and azide or cyanate are heated in dimethyl sulfoxide at 60 °C. During this reaction, 0.5 mol of N_2O is evolved/mol of dinitrosyl complex, and compounds of the type $(Et_4N)[MoL_2(R_2dtc)_2NO]$ (L = N_3, NCO) have been isolated.[1,3] The ^{15}N-labeling studies have shown that the N_2O originates entirely from the nitrosyl groups and, moreover, that only one nitrosyl group per molecule reacts via an intermolecular mechanism. The same type of nitrosyl reactivity has also been observed for *cis*-$W(Et_2dtc)_2(NO)_2$, although in this case, the reaction requires photochemical activation in order to proceed.[4]

The rate-determining step in the proposed reaction mechanism[1] involves the anion coordinating to the "18-electron" *cis*-$M(R_2dtc)_2(NO)_2$ to give the reactive seven-coordinate intermediate $ML(R_2dtc)_2(NO)_2^-$. Rather than a formulation of this as an energetically unfavorable "20-electron" species, it was suggested that the anion coordination be accompanied by the transfer of an electron pair from the metal to a nitrosyl-based molecular orbital (MO). In this paper we describe electrochemical and ESR experiments which demonstrate the existence of this MO. UV–visible and IR spectral data for the *cis*-$M(R_2dtc)_2(NO)_2$ complexes are also presented and discussed in terms of the metal–dinitrosyl moiety interaction.

Experimental Section

Materials. The preparations of the $Mo(R_2dtc)_2(NO)_2$ and $W(Et_2dtc)_2(NO)_2$ complexes have been described previously.[5] All solvents were AR grade and were used without further purification.

Electrochemistry. The electrochemical measurements were performed at room temperature (~22 °C) with use of PAR Model 170 instrumentation. Measurements were carried out in dinitrogen-saturated acetone solutions, 0.1 M in tetraethylammonium perchlorate, by using a three-electrode *iR*-compensated system. The working electrode for the cyclic and ac voltammetry was a platinum-disk electrode with a geometrical area of 0.27 cm^2. The reference and auxiliary electrodes were respectively Ag|AgCl|0.1 M LiCl and platinum.

The ac voltammograms were recorded at 10 mV/s by using an 80-Hz, 5-mV peak-to-peak perturbation and a phase angle of 90° with respect to the applied alternating potential. Cyclic voltammograms were obtained with a scan rate of 100 mV/s. Controlled-potential coulometry on *cis*-$Mo(Et_2dtc)_2(NO)_2$ was carried out at −0.8 V.

Electron Spin Resonance Spectra. X-Band electron spin resonance (ESR) spectra were obtained by using a JEOL PES-3 spectrometer in acetone solution at 25 °C and in frozen solution between −160 and −170 °C. The radial anions $Mo(R_2dtc)_2(NO)_2^-$ were generated in situ in cylindrical quartz ESR tubes with use of a cylindrical gold coil working electrode by following a modification of the design of Allendorfer,[6] Figure 1. Acetone solutions of the complexes were electrolyzed at potentials greater than the reduction potential of the complex, which was determined by voltammetric methods within the cell, typically −0.8 V vs. Ag|AgCl|0.1 M LiCl. The solution spectra then obtained were of the reduced complex in the thin film of solution between the gold coil and the quartz ESR tube. Frozen-solution spectra were recorded by cooling the ESR tube in the JEOL variable-temperature attachment.

Simulation of Frozen-Solution ESR Spectra. In frozen solutions all orientations of the complex with respect to the applied field are present. It is then necessary to calculate the ESR line shape by integration over all orientations to yield a line shape function

$$f(H) = \sum_{K=1}^{u} \int_{\phi} \int_{\theta} P(K,\theta,\phi)\, G(H,K,\theta,\phi)\, d\cos\theta\, d\phi \qquad (1)$$

where u is the number of transitions, $P(K,\theta,\phi)$ is the transition probability of the Kth transition, and $G(H,K,\theta,\phi)$ is the first-derivative component line shape. In simulations here, P consisted only of a term representing the effect of **g** tensor anisotropy[7] while the first-derivative component line shapes were taken as the appropriate normalized Gaussian first derivatives $G(H,K,\theta\phi) = -(H - H(K,\theta,\phi))/\sigma^3) \exp((H - H(K,\theta,\phi))^2/2\sigma^2)$[8] where $H(K,\theta,\phi)$ is the transition field of the Kth transition of a complex for which H makes polar angles θ and ϕ with the x, y, and z axes. The line shape integral was evaluated numerically by following the method of Smith and Pilbrow[9] by the summation

$$f(H) = \sum_{K=1}^{u} \sum_{\phi} \sum_{\theta} P(K,\theta,\phi)\, G(H,K,\theta,\phi)\, \Delta\cos\theta\, \Delta\phi \qquad (2)$$

(1) Broomhead, J. A.; Budge, J. R. *Inorg. Chem.* **1978**, *17*, 2414.
(2) Abbreviations: (a) Chemical: R_2dtc, N,N-disubstituted dithiocarbamate; Bzl, benzyl; pyr, pyrrolidyl. (b) Ac voltammetry: E_{dc}, the dc component of the applied potential; $E_{1/2}$, the reversible half-wave potential; I_p, ac current at the peak maximum; n, number of electrons involved in the electrochemical process; E_p, peak potential of the ac voltammogram. (c) Cyclic voltammetry: ΔE_p the peak separation in the cyclic voltammogram; C, concentration in M; v, scan rate in mV s^{-1}. (d) Molecular orbital calculations: a_p, the coefficient of the nitrogen p_π orbital in the molecular orbital occupied by the unpaired electron. All other symbols are those commonly employed.
(3) Broomhead, J. A.; Budge, J. R.; Grumley, W. D.; Norman, T. R.; Sterns, M. *Aust. J. Chem.* **1976**, *29*, 275.
(4) Broomhead, J. A.; Budge, J. R. *Aust. J. Chem.* **1979**, *32*, 1187.
(5) Broomhead, J. A.; Budge, J. R.; Grumley, W. *Inorg. Synth.* **1976**, *16*, 235.
(6) Allendoerfer, R. D.; Martinchek, G. A.; Bruckenstrin, S. *Anal. Chem.* **1975**, *47*, 890.
(7) Pilbrow, J. R. *Mol. Phys.* **1969**, *16*, 307.
(8) Boas, J. F.; Dunhill, R. H.; Pilbrow, J. R.; Srivastava, R. C.; Smith, T. D. *J. Chem. Soc. A* **1969**, 94.

0020-1669/82/1321-1031$01.25/0

Table I. Cyclic and Ac Voltammetric Parameters for the Reduction of *cis*-$M(R_2dtc)_2(NO)_2$ Complexes

	ac voltammetry				cyclic voltammetry		
compd	E_p, V	$\Delta E/2$, mV	slope,[a] mV	I_p/C, mA M^{-1}	i_p^f/i_p^b [b]	ΔE_p, mV	$i_p^f/CV^{1/2}$, mA $s^{-1/2}$ M^{-1} $mV^{-1/2}$
$Mo(Me_2dtc)_2(NO)_2$	−0.626	97	125	52	1.02	68	11.4
$Mo(Et_2dtc)_2(NO)_2$	−0.642	95	122	58	1.06	64	10.7
$Mo((pyr)dtc)_2(NO)_2$	−0.634	100	132	54	0.98	72	9.8
$Mo(i\text{-}Pr_2dtc)_2(NO)_2$	−0.680	100	131	48	1.03	67	10.1
$Mo(n\text{-}Bu_2dtc)_2(NO)_2$	−0.648	103	131	45	1.03	65	9.7
$Mo(Bzl_2dtc)_2(NO)_2$	−0.566	98	129	51	1.00	63	8.6
$W(Et_2dtc)_2(NO)_2$	−0.733	99	130	57	0.97	63	9.6

[a] The slope of the plot of E_{dc} vs. ln $[(I_p/I)^{1/2} \pm (I_p - I)/I)^{1/2}]$. [b] The ratio of i_p^f/i_p^b was calculated according to ref 31.

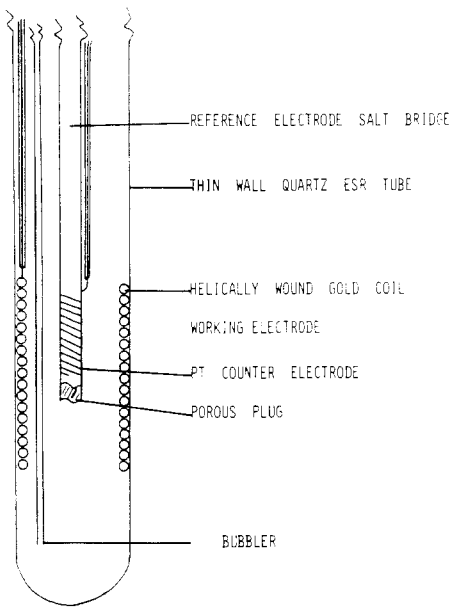

Figure 1. In situ ESR electrolysis cell.

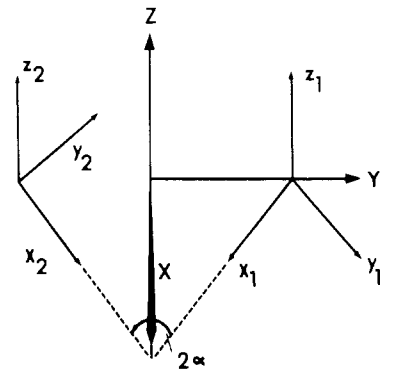

Figure 2. Principal axes of the **g**(x, y, z) and nitrogen nuclear hyperfine $(x_1, y_1, z_1; x_2, y_2, z_2)$ interactions for $M(R_2dtc)_2(NO)_2^-$. The x_1 and x_2 directions lie along NO bonds.

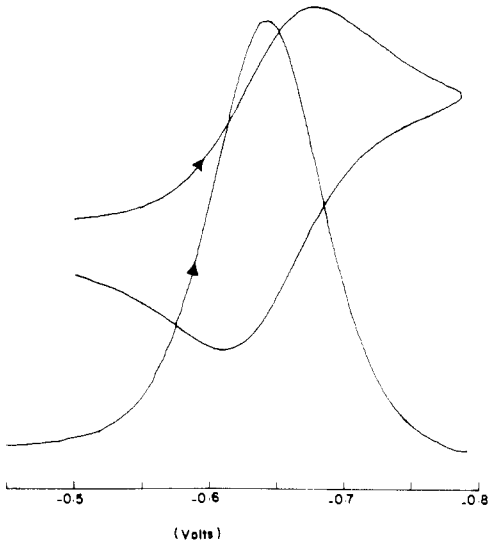

Figure 3. Cyclic and ac voltammograms for the one-electron reduction of *cis*-$Mo(Et_2dtc)_2(NO)_2$ in acetone (0.1 M in tetraethylammonium perchlorate).

and by taking sufficient orientations of θ and ϕ. For monoclinic symmetry it is necessary to sum over angles θ = 0–90° and ϕ = 0–180°. Isotropic line widths σ were used. The spin Hamiltonian used to describe the system was of monoclinic (C_2) symmetry with the principal directions of the **g** tensor along the directions x, y, and z indicated in Figure 2 and the principal axes of the nuclear electron hyperfine interaction tensors along (x_1, y_1, z_1) and (x_2, y_2, z_2), respectively. The spin Hamiltonian describing such a system is of the form[10]

$$H = \beta[g_xG_xS_x + g_yH_yS_y + g_zH_zS_z] + A_{x_1}I_{x_1}S_{x_1} + A_{y_1}I_{y_1}S_{y_1} + A_{z_1}I_{z_1}S_{z_1} + A_{x_2}I_{x_2}S_{x_2} + A_{y_2}I_{y_2}S_{y_2} + A_{z_2}I_{z_2}S_{z_2} \quad (3)$$

In the case of two equivalent nitrogen atoms $A_{x_1} = A_{x_2}$, $A_{y_1} = A_{y_2}$, and $A_{z_1} = A_{z_2}$. $I_1 = I_2 = {}^1/_2$ for $(Mo(Et_2dtc)_2(^{15}NO)_2^-$, and $I_1 = I_2 = 1$ for $Mo(Et_2dtc)_2(NO)_2^-$. Such a spin Hamiltonian has monoclinic symmetry due to the noncoincidence of the principal axes of the **g** and nuclear electron hyperfine interaction terms.[11] The spin Hamiltonian was solved to obtain the transition fields for both the NO and ^{15}NO complexes by conventional methods.[12] The **g** tensor was transformed to the Zeeman representation[13] and nuclear electron hyperfine interaction included to first order[14] (a reasonable approximation in view of the relative magnitudes of g_{iso} and A_{iso}). This then led to four transition fields for the ^{15}NO complex and nine transition fields for the NO complex. Best-fit simulated spectra were obtained for both the ^{15}NO and NO complexes by direct comparison of the experimental spectra with line shapes calculated for a wide variety of **g** and hyperfine parameters. A particular problem in this procedure is the lack of resolution, particularly of the hyperfine features for the smaller hyperfine parameters; however, limits may be put on allowable values of these parameters.

Infrared and visible spectra were recorded on Unicam SP200G and Cary 214 spectrophotometers, respectively. For solution infrared studies, a sample of $Mo(Et_2dtc)_2(NO)_2$ in dichloromethane, saturated with tetraethylammonium perchlorate, was reduced electrochemically under dinitrogen. Some of the solution was then transferred to an infrared cell and the spectrum recorded. For this solvent system, the infrared spectral region between 2000 and 1500 cm^{-1} was free of any strong absorptions due to background electrolyte or solvents.

(9) Smith, T. D.; Pilbrow, J. R. *Coord. Chem. Rev.* **1974**, *13*, 173.
(10) Pilbrow, J. R.; Winfield, M. E. *Mol. Phys.* **1973**, *25*, 1073.
(11) Kneubühl, F. K. *Phys. Kondens. Mater.* **1963**, *1*, 410.
(12) Abragam, A.; Bleaney, B. "Electron Paramagnetic Resonance of Transition Ions"; Oxford University Press: London, 1970; p 135.
(13) Atherton, N. M. "Electron Spin Resonance"; Ellis Harwood: 1973; p 122.
(14) Carrington, A.; McLachlan, A. D. "Introduction to Magnetic Resonance"; Harper and Row: New York, 1969; Chapter 7.

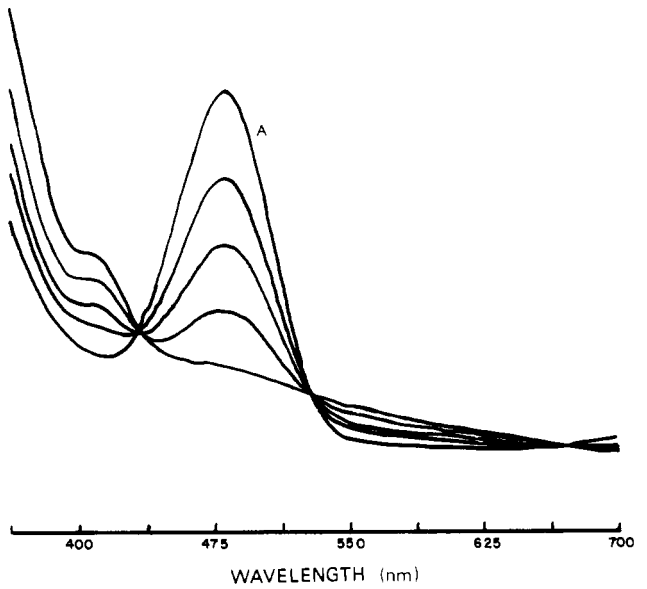

Figure 4. Changes occurring in the UV–visible spectrum during the exhaustive electrolysis of $Mo(Et_2dtc)_2(NO)_2$ in acetone (0.1 M tetraethylammonium perchlorate). A = initial trace, with successive traces at 25%, 50%, 75%, and 100% conversion to $Mo(Et_2dtc)_2(NO)_2^-$.

Results and Discussion

Electrochemistry. The cyclic and ac voltammograms obtained for *cis*-$Mo(Et_2dtc)_2(NO)_2$ are shown in Figure 3 while Table I summarizes the electrochemical parameters for each of the *cis*-$Mo(R_2dtc)_2(NO)_2$ complexes studied. All of the dinitrosyl compounds show a reduction process occurring between −0.566 and −0.733 V. Controlled-potential coulometry on *cis*-$Mo(Et_2dtc)_2(NO)_2$ has shown that 1 mol of electrons is consumed/mol of complex. The spectral changes accompanying the reduction of *cis*-$Mo(Et_2dtc)_2(NO)_2$ are shown in Figure 4. No other oxidation or reduction process was observed over the range +1.5 to −1.3 V. The electrochemical data (Table I) suggest that each of the *cis*-$Mo(R_2dtc)_2(NO)_2$ complexes undergo a similar one-electron reduction, and consequently, only the R = Et case will be discussed in any detail.

Equation 4, describing the ac wave for a reversible elec-

$$E_{dc} = E_{1/2} + \frac{2RT}{nF} \ln \left[\left(\frac{I_p}{I} \right)^{1/2} - \left(\frac{I_p - I}{I} \right)^{1/2} \right] \quad (4)$$

tron-transfer process and the half-height width of the ac wave, where $\Delta E/2 = 90/n$ mV at 25 °C, is used as a diagnostic test for reversibility. The entire wave may also be analyzed by plotting E_{dc} vs. ln $[(I_p/I)^{1/2} \pm (I_p - I/I)^{1/2}]$, for reversible processes the slope should equal $118/n$ mV at 25 °C.[15] The experimentally determined slope for *cis*-$Mo(Et_2dtc)_2(NO)_2$ of 122 mV and the half-height width of 98 mV, therefore, closely approach those expected for a reversible one-electron transfer. *cis*-$Mo(Et_2dtc)_2(NO)_2$ also gives cyclic voltammograms centered at −0.646 V, with 64-mV peak separations, at scan rates up to 200 mV/s and with a ratio of "forward" cathodic to "back" anodic peak currents (i_p^f/i_p^b) of 1.06. This is again consistent with (5) being reversible.[15]

$$Mo(Et_2dtc)_2(NO)_2 + e^- \rightleftharpoons [Mo(Et_2dtc)_2(NO)_2]^- \quad (5)$$

The effect of the dithiocarbamate substituents on the reduction potentials of the *cis*-$Mo(R_2dtc)_2(NO)_2$ complexes follows a similar pattern to that observed for iron and manganese dithiocarbamate complexes.[16,17] The ease of reduction of the *cis*-$Mo(R_2dtc)_2(NO)_2$ complexes is in the order Bzl ≫ Me > pyr > Et > *n*-Bu > *i*-Pr.

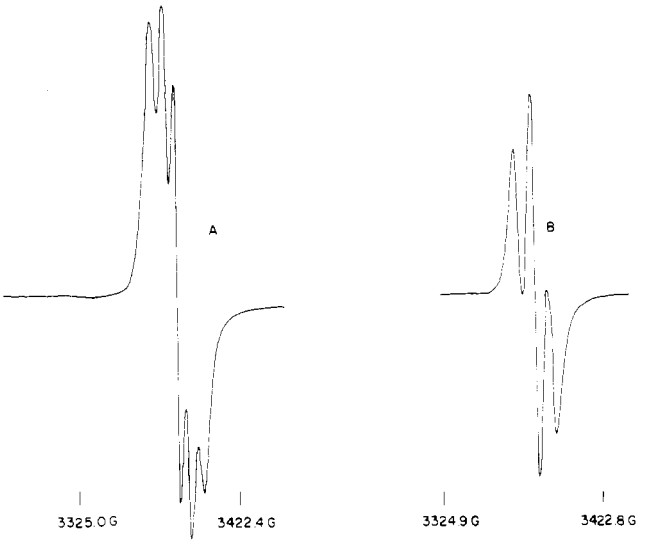

Figure 5. Isotropic solution ESR spectra of (A) $[Mo(Et_2dtc)_2(NO)_2]^-$ and (B) $[Mo(Et_2dtc)_2(^{15}NO)_2]^-$, in acetone (0.1 M in tetraethylammonium perchlorate).

Table II. ESR Data on *cis*-$M(R_2dtc)_2(NO)_2$ Complexes

compd	isotropic spectra	
	g_{av}	N hyperfine coupling, G
$Mo(Et_2dtc)_2(NO)_2$	2.0075	7.6
$Mo(Et_2dtc)_2(^{15}NO)_2$	2.0064	10.2
$Mo(i\text{-}Pr_2dtc)_2(NO)_2$	2.0072	7.5
$Mo(Bzl_2dtc)_2(NO)_2$	2.0071	7.4
$W(Et_2dtc)_2(NO)_2$	2.0191	

Solution ESR Spectra. For some understanding of the nature of the radical anions $M(S_2CNR_2)_2(NO)_2^-$, the ESR spectra of some of these species were investigated. Figure 5 shows the isotropic solution ESR spectra of $Mo(Et_2dtc)_2(NO)_2^-$ and $Mo(Et_2dtc)_2(^{15}NO)_2^-$. The five-line spectrum in the former (Figure 5A) reduces to three lines in the latter (Figure 5B) and therefore confirms that the hyperfine splittings are due to the unpaired electron interacting equally with the two nitrosyl nitrogen atoms. Similar spectra were observed for the other molybdenum complexes, and Table II summarizes the data for the solution ESR spectra. The solution spectrum of $W(Et_2dtc)_2(NO)_2^-$ consisted of a broad line centered on g = 2.019. with no resolution of nitrogen hyperfine lines.

The solution ESR spectra strongly suggest that the unpaired electron in $M(R_2dtc)_2(NO)_2^-$ complexes is associated with a nitrosyl-based molecular orbital that is delocalized equally over both NO groups. There appears in the spectra of both the molybdenum and tungsten complexes to be no evidence of metal nuclear hyperfine interaction from either 15.72% ^{95}Mo ($I = {}^5/_2$) and 9.46% ^{97}Mo ($I = {}^5/_2$) or 14.4% ^{183}W ($I = {}^1/_2$).[18a] The nonresolution of the metal hyperfine coupling puts a possible upper limit on the isotropic metal hyperfine interaction

(15) (a) Bond, A. M. *Anal. Chem.* **1972**, *44*, 315. (b) Brown, E. R.; Large, R. F. In "Physical Methods of Chemistry"; Weissberger, A.; B. W., Rossiter, Eds.; Wiley-Interscience: New York, 1971; Part IIA.

(16) Hendrickson, A. R.; Martin, R. L.; Rohde, N. M. *Inorg. Chem.* **1974**, *13*, 1933.

(17) Chant, R. L.; Hendrickson, A. R.; Martin, R. L.; Rohde, N. M. *Inorg. Chem.* **1975**, *14*, 1894.

(18) (a) Typical molybdenum isotropic hyperfine coupling constants are in the range 10–60 G. (For example, for $Mo(V)(Me_2dtc)_4^+$, A_{iso} = 34.5 G: Hyde, J.; Zubieta, J. *J. Inorg. Nucl. Chem.* **1977**, *39*, 289.) (b) This may be compared with molybdenum(V) complexes with coordinated nitrogen such as Mo(V) thio–imino complexes where $A_{iso}(Mo)$ = 38 G and $A_{iso}(N)$ = 2.1 G: Gardener, J. K.; Pariyadath, N.; Corbin, J. L.; Stiefel, E. I. *Inorg. Chem.* **1978**, *17*, 897.

Table III. Anisotropic g and Nuclear Hyperfine Tensors for *cis*-$Mo(Et_2dtc)_2(NO)_2^-$

compd	g_x (±0.001)	g_y (±0.001)	g_z (±0.001)	g_{av}	10^4 cm^{-1} A_x (±1)	A_y (±1)	A_z (±1)	A_{av}	2α (±5), deg
$Mo(Et_2dtc)_2(^{15}NO)_2^-$	1.995	2.011	2.012	2.006	4	22	4	10	85
$Mo(Et_2dtc)_2(NO)_2^-$	1.995	2.011	2.012	2.006	3	16	3	7.3	85

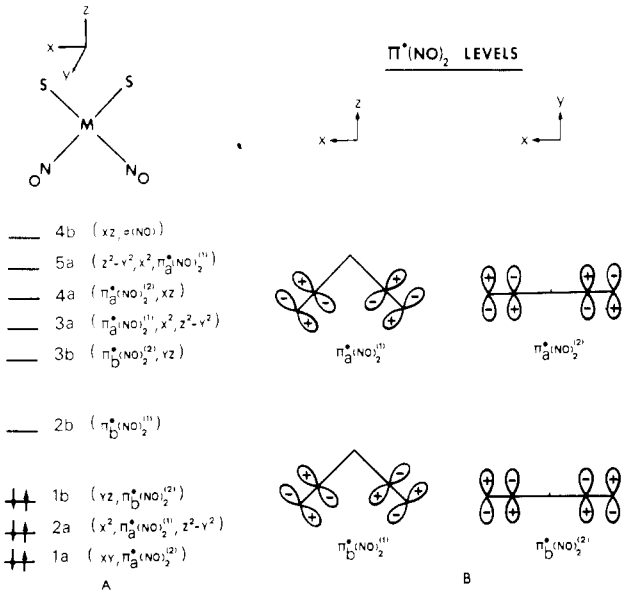

Figure 6. (A) Molecular orbital scheme for *cis*-$M(R_2dtc)_2(NO)_2$. (B) The π^* $(NO)_2$ orbitals.

of ~2 G. The magnitude of the nitrogen isotropic hyperfine coupling, ~7.5 G, taken together with the small metal hyperfine coupling, indicates that the singly occupied LUMO makes only a small metal contribution.[18b] The isotropic *g* values obtained for the molybdenum dinitrosyl anions are almost identical, i.e., virtually independent of the dithiocarbamate substituent.

These observations are in agreement with the qualitative molecular orbital scheme proposed for this type of complex (Figure 6).[19] The *cis*-$M(R_2dtc)_2(NO)_2$ compounds are six-coordinate $\{M(NO)_2\}^6$ systems with C_2 symmetry. The three lower energy metal-based orbitals 1a, 2a, and 1b are occupied while the relatively low-lying orbital 2b is the LUMO of the molecule. This MO is equally delocalized over each of the nitrosyl groups and is expected to have minimal metal d-orbital character.[19] The one-electron reduction of *cis*-$M(R_2dtc)_2(NO)_2$ would then, in this molecular orbital scheme, place an electron into the 2b LUMO, giving an electron configuration $(1a)^2(2a)^2(1b)^2(2b)^1$.

Frozen-solution ESR spectra for $Mo(Et_2dtc)_2(^{15}NO)_2^-$ and $Mo(Et_2dtc)_2(NO)_2^-$ are shown in Figure 7. A complex, but different, line shape was observed for the two species, indicating that anisotropic nitrogen hyperfine coupling was resolved at least in part together with the effects due to anisotropy of the **g** tensor. A less well-resolved spectrum was obtained for a frozen solution of $W(Et_2dtc)_2(NO)_2^-$, which has features similar to those observed for $Mo(Et_2dtc)_2(NO)_2^-$.

An analysis of the frozen-solution ESR spectra of both $Mo(R_2dtc)_2(NO)_2^-$ and $Mo(R_2dtc)_2(^{15}NO)_2^-$ complexes allows further verification of the nature of the LUMO occupied by the unpaired electron. The symmetry of the molecule is low (C_2). However, on consideration of the $Mo(NO)_2$ group over which the LUMO is delocalized, it is possible to use the nearly C_{2v} symmetry of this group to estimate the principal directions

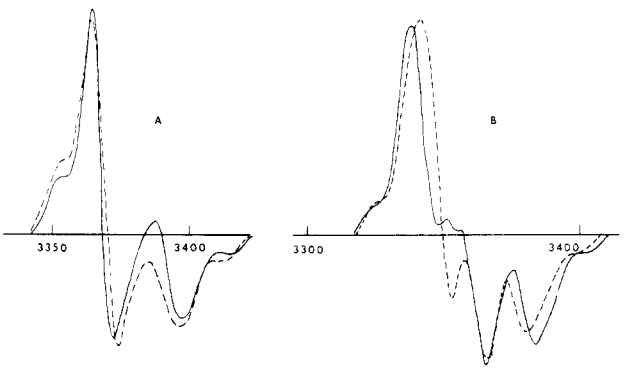

Figure 7. Observed (—) and calculated (---) ESR spectra of frozen acetone solutions (0.1 M tetraethylammonium perchlorate) of (A) $Mo(Et_2dtc)_2(^{15}NO)_2^-$ at 9.490 GHz and (B) $Mo(Et_2dtc)_2(NO)_2^-$ at 9.438 GHz. Parameters used for the calculated spectra are those given in Table III; component line widths are 3.5 G.

of the **g** tensor. The system then has monoclinic symmetry due to a noncoincidence of the principle axes of the **g** and nitrogen hyperfine tensors. This will occur because for the orbital the nitrogen p_π orbitals lie in the plane of the $(NO)_2$ group perpendicular to the N–O direction.[19] The dipolar coupling between the electron in the p_π orbital and the nuclear spin leads to an axial hyperfine tensor for each nitrogen with the "parallel" (y_1, y_2) axes along the direction of the *p*-orbital lobes.[21] The perpendicular axes are chosen to lie in the $(NO)_2$ plane (x_1, x_2) and perpendicular to it (z_1, z_2).[22] With use of the C_{2v} symmetry of the $Mo(NO)_2$ moiety, that is, with the effect of other ligands bound to the molybdenum atom considered to have little influence on the (2b) Π MO, principal axis directions of the **g** tensor (x, *y*, *z*) are determined by the C_{2v} symmetry elements.

Simulations of the frozen-solution spectra were performed by using a spin Hamiltonian (eq 3) appropriate to the symmetry of the $(2b)^1$ π radical. The hyperfine interaction was taken as axial on each nitrogen atom ($A_{x_1} = A_{z_1}$), with the values of the principal components restricted so that their average was equal to the solution hyperfine coupling constant. The principal values of the **g** tensor were similarly restricted such that their average was equal to the solution-determined *g* value. The spectrum of $Mo(Et_2dtc)_2(^{15}NO)_2^-$ was found to be well reproduced (Figure 7A) for the spin-Hamiltonian parameters shown in Table III. The error limits were determined by the change required in any of the parameters sufficient to cause a significant alteration in the simulated spectrum. Figure 8 shows the variation of simulated spectra for variations in the angle 2α between the two "parallel" axes of the nitrogen hyperfine interaction. With use of the *g* values determined for the ^{15}NO complex, a best-fit spectrum was computed for $Mo(Et_2dtc)_2(NO)_2^-$ (Figure 7B). The values of the spin-Hamiltonian parameters for the best fit, together with an estimate of errors, are given in Table III. It was not possible to reproduce every feature of the ^{14}NO spectrum, particularly in the 3350-G region. This is partly due to a lack of resolution in the spectrum where a considerable number of

(19) Enemark, J. H.; Feltham, R. D. *Coord. Chem. Rev.* **1976**, *15*, 2970.
(20) Martin, R. L.; Taylor, D. *Inorg. Chem.* **1976**, *15*, 2970.
(21) Symons, M. "Chemical and Biochemical Aspects of Electron-Spin Resonance Spectroscopy"; Wiley: New York, 1978; Chapter 4.
(22) The choice of direction of the perpendicular axes is arbitrary for an axial hyperfine tensor as considered here.

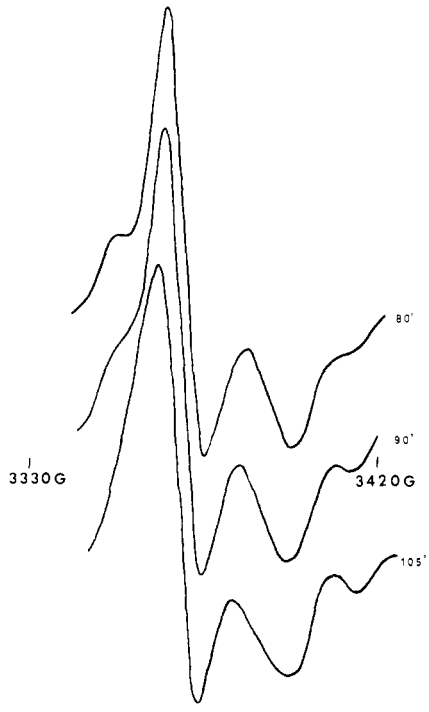

Figure 8. Simulated "frozen" ESR spectra of $Mo(Et_2dtc)_2(^{15}NO)_2^-$ calculated for $g_x = 1.995$, $g_y = 2.011$, $g_z = 2.001$, $A_x = 4 \times 10^{-4}$ cm^{-1}, $A_y = 22 \times 10^{-4}$ cm^{-1}, $A_z = 4 \times 10^{-4}$ cm^{-1}, and 2α values of 80, 90, and 105°.

ESR transitions from molecules with the field in the *yz* plane overlap. Thus there is greater uncertainty in the spin-Hamiltonian parameters for $Mo(Et_2dtc)_2(NO)_2^-$.

The lack of resolution for the corresponding tungsten complex is due to the increased line width in both the solution and frozen-solution spectra. The origin of the increase in line width may be attributed to the increase in the spin–orbit coupling constants of tungsten and molybdenum, leading to an increase in the efficacy of the relaxation mechanism. The features of the frozen-solution spectra however indicate that a similar species (based on the nitrosyl LUMO 2b) is formed on reduction.

Nitrogen Atom Spin Densities. It is not possible to determine the sign of either the isotropic or anisotropic components of the hyperfine tensor from these experiments. For a π radical such as considered here, the values of the hyperfine tensors for the ^{15}NO and NO complexes lead to consistent spin densities on the nitrogen atoms for each species if the following are true: (1) The isotropic hyperfine interaction is due to spin polarization[23] of the nitrogen s electrons by the unpaired electron in a nitrogen p_π orbital. This would lead to a negative sign for the isotropic ^{15}N hyperfine constant ($A(^{15}N)$) and a positive sign for the N hyperfine constant ($A(N)$).[24] (2) The anisotropic hyperfine interaction is due to dipolar coupling.[21] The signs of the anisotropic components would then be negative for the ^{15}NO complex and positive for the NO complex.

The nitrogen p-orbital population (a_p^2) may be estimated from the calculated dipolar contribution to the components of the hyperfine tensor, by using the relationship $a_p^2 = 2B/B_0$,[25] where B and B_0 are respectively the dipolar hyperfine coupling and the dipolar hyperfine coupling for unit occupation of the nitrogen p orbital. The orbital populations calculated for the ^{15}NO and NO complexes are respectively 0.25 and 0.26.[26] The agreement between the orbital populations is gratifying and well within the errors of estimation of the nitrogen hyperfine coupling constants.

Table IV. Nitrosyl Stretching Frequencies

compd	ν(NO), cm^{-1} [a]	ref
$Mo(Me_2dtc)_2(NO)_2$	1657, 1767	this work[c]
$Mo(Et_2dtc)_2(NO)_2$	1654, 1765	this work[d]
$Mo((pyr)dtc)_2(NO)_2$	1657, 1768	this work
$Mo(i\text{-}Pr_2dtc)_2(NO)_2$	1646, 1760	this work
$Mo(n\text{-}Bu_2dtc)_2(NO)_2$	1651, 1764	this work
$Mo(Bzl_2dtc)_2(NO)_2$	1659, 1768	this work
$Mo(Et_2dtc)_2(NO)_2^-$	1570, ?[e]	this work
$W(Me_2dtc)_2(NO)_2$	1635, 1740	ref 32
$W(Et_2dtc)_2(NO)_2$	1632, 1739	this work
$Cr(Et_2dtc)_2(NO)_2$	1660, 1785[b]	ref 31

[a] In $CHCl_3$, unless otherwise stated. [b] KBr disk. [c] 1650 m, 1765 cm^{-1} according to ref 33. [d] 1655, 1775 cm^{-1} according to ref 33. [e] In CH_2Cl_2 saturated with tetraethylammonium perchlorate.

Magnitude of the Monoclinic Angle 2α. It is of interest to compare the angle (2α) between the principal axes of the nitrogen hyperfine interaction with the angle between the NO vectors in $Mo(Et_2dtc)_2(NO)_2$[27] of 81.5°. The "parallel" *y* axes of the two NO groups are perpendicular to the NO directions for an electron occupying the 2b orbital, and hence the angle between these two axes will be related to the angle between the NO groups. Analysis of the frozen-solution spectra leads to a value of 2α of 85 ± 5°. Outside these limits it is not possible to satisfactorily reproduce the experimental spectra by simulation and minor changes in structure that may accompany the reversible one-electron reduction cannot be detected.

Infrared and UV–Visible Spectra. Table IV gives the nitrosyl stretching frequencies for the *cis*-$M(R_2dtc)_2(NO)_2$ complexes. For M = Mo, it is apparent that the nitrosyl stretching frequencies are relatively insensitive to the electron-donating capacities of the various dithiocarbamate ligands. However, for the series *cis*-$Cr(Et_2dtc)_2(NO)_2$, *cis*-$Mo(Et_2dtc)_2(NO)_2$, and *cis*-$W(Et_2dtc)_2(NO)_2$, the ν(NO)'s decrease in accord with an increasing metal–dinitrosyl moiety interaction. The reduced radical anion $Mo(Et_2dtc)_2(NO)_2^-$ has a nitrosyl stretching frequency at 1570 cm^{-1} in dichloromethane saturated with tetraethylammonium perchlorate. There may be an additional nitrosyl band at lower frequency, but the region is obscured by strong solvent bands. Upon aerial oxidation of the above solution, the 1570-cm^{-1} band disappears and the nitrosyl bands due to *cis*-$Mo(Et_2dtc)_2(NO)_2$ appear. Presumably dioxygen is reduced to superoxide in this process, but we have not specifically looked for the dioxygen reduction product.

The UV–visible spectra of the dinitrosyl complexes between 2600 and 8000 Å (Table V) show three absorption bands, and for convenience these have been labeled A, B, and C. For the diethyldithiocarbamate complexes of Cr, Mo, and W, bands A and C appear virtually independent of the metal, whereas band B shifts from 5120 Å in *cis*-$Cr(Et_2dtc)_2(NO)_2$ to 4850 Å to *cis*-$Mo(Et_2dtc)_2(NO)_2$ and to 4615 Å in *cis*-$W(Et_2dtc)_2(NO)_2$. Also, in comparing the various molybdenum complex spectra, we note that band C is particularly sensitive to the type of dithiocarbamate substituent present while bands A and B are affected to a lesser extent. In addition, with the

(23) Bolton, J. R. "Radical Ions"; Wiley: New York, 1968; Chapter 7.
(24) The values of the hyperfine coupling constant for unit population of the S atomic orbitals are +555.1 G for ^{14}N and −778.7 G for ^{15}N (Froese, C. *J. Chem. Phys.* **1966**, *45*, 1417).
(25) Atkins, P. W.; Symons, M. C. R. "The Structure of Inorganic Radicals"; Elsevier: Amsterdam, 1967.
(26) The nitrogen dipolar hyperfine coupling was calculated from $A_{11} = A_{iso} + 2B$ and $A_\perp = A_{iso} - B$. The values obtained were $2B(^{15}N) = 12 \times 10^{-4}$ cm^{-1}, $-B(^{15}N) = 6 \times 10^{-4}$ cm^{-1} and $2B(N) = 9 \times 10^{-4}$ cm^{-1}, $-B(N) = 4 \times 10^{-4}$ cm^{-1}.
(27) Broomhead, J. A.; Budge, J. R.; Sterns, M.; White, A. H. *Aust. J. Chem.*, in press.

Table V. UV-Visible Spectra

compd[a]	solvent	band A[b]	band B[b]	band C[b]
$Mo(Bzl_2dtc)_2(NO)_2$ (−0.567 V)	$CHCl_3$	2830 (2.65×10^4)	4770 (2.42×10^3)	7140 (1.41×10^2)
$Mo(Me_2dtc)_2(NO)_2$ (−0.626 V)	MeOH	2720 (2.37×10^4)	4795 (2.24×10^3)	...
	$CHCl_3$	...	4755	6990 (1.13×10^2)
$Mo(Pyr_2dtc)_2(NO)_2$ (−0.634 V)	MeOH	2740 (2.64×10^4)	4792 (2.32×10^3)	...
	$CHCl_3$	...	4760	7080 (1.21×10^2)
$Mo(Et_2dtc)_2(NO)_2$ (−0.642 V)	MeOH	2740 (2.44×10^4)	4805 (2.26×10^3)	...
	$CHCl_3$	...	4785	7130 (1.33×10^2)
$Mo(n\text{-}Bu_2dtc)_2(NO)_2$ (−0.648 V)	MeOH	2760 (2.51×10^4)	4810 (2.30×10^3)	...
	$CHCl_3$	...	4790	7150 (1.38×10^2)
$Mo(i\text{-}Pr_2dtc)_2(NO)_2$ (−0.680 V)	MeOH	2780 (2.38×10^4)	4842 (2.51×10^3)	...
	$CHCl_3$	...	4830	7220 (1.46×10^2)
$W(Et_2dtc)_2(NO)_2$ (−0.733 V)	MeOH	2720 (1.66×10^4)	4615 (2.93×10^3)	...
	$CHCl_3$	...	...	7140 (1.58×10^2)
$Cr(Et_2dtc)_2(NO)_2$[c]	EtOH	2730 (3×10^4) 3000 sh (1.3×10^4)	5120 (1.7×10^3)	7190 (0.8×10^2)

[a] The reduction potential is shown in parentheses after each compound. [b] Wavelengths are given in angstroms. Extinction coefficients are shown in parentheses. ... indicates that the peak position was not determined. [c] Reference 32.

exception of the benzyl substituent, there is a trend toward longer wavelengths for each of the bands (A, B, and C) with the increasing electron-donating capacity of the dithiocarbamate.

The above results are consistent with bands A and C being dithiocarbamate based, but it is difficult to make more definite assignments due to the limited information available on the electronic spectra of dithiocarbamate complexes.[28] On the other hand, the position of band B is dependent on the metal present, and we have assigned it to the 1b → 2b transition—see Figure 6. The trend to shorter wavelengths observed for band B on going from Cr to W accords with an increase in energy for this transition.

Conclusion

Electrochemical and ESR studies of the one-electron reduction of *cis*-$Mo(R_2dtc)_2(NO)_2$ and *cis*-$W(R_2dtc)_2(NO)_2$ demonstrate the existence of an energetically accessible dinitrosyl-based molecular orbital as the LUMO. This molecular orbital is delocalized over the nitrosyl groups and possesses little or no metal orbital character. The present work provides good experimental evidence for the delocalized π^* $(NO)_2$ levels that have been used by Enemark and Feltham[19] and Martin and Taylor[20] to rationalize the various dinitrosyl geometries observed for the pseudotetrahedral $ML_2(NO)_2^{n+}$ complexes (L = variety of different ligands).

The reactions of the *cis*-$Mo(R_2dtc)_2(NO)_2$ complexes with azide and cyanate have been discussed previously in terms of the MO scheme shown in Figure 6. The tungsten complex, *cis*-$W(Et_2dtc)_2(NO)_2$, is considerably less reactive, and this may be attributed in part to the larger energy required to transfer an electron pair from the metal d orbitals in the π_b^* $(NO)_2$[(1)] orbital upon formation of a postulated "reactive seven-coordinate intermediate".

Reversible one-electron reductions have been reported for the mononitrosyl complexes $Fe(CN)_5NO^{3-}$, $RuCl(bpy)NO^{2+}$, and $Fe(S_2C_2R_2)_2NO^-$,[29,30] and ESR studies have indicated that these reductions are nitrosyl based. However, no reports have appeared that show the one-electron reduction of a dinitrosyl group as is observed for *cis*-$M(R_2dtc)_2(NO)_2$ complexes. Further, the $M(R_2dtc)_2(NO)_2^-$ species are to our knowledge *the first well-characterized examples of six-coordinated* $\{M(NO)_2\}^7$ *systems*.

Acknowledgment. P.D.W.B. acknowledges the receipt of a Queen Elizabeth II Fellowship at the Research School of Chemistry, ANU. Mrs. Janet Hope is thanked for technical assistance.

Registry No. $Mo(Me_2dtc)_2(NO)_2$, 26087-84-3; $Mo(Et_2dtc)_2(NO)_2$, 39797-80-3; $Mo((pyr)dtc)_2(NO)_2$, 66793-34-8; $Mo(i\text{-}Pr_2dtc)_2(NO)_2$, 66793-36-0; $Mo(n\text{-}Bu_2dtc)_2(NO)_2$, 66793-35-9; $Mo(Bzl_2dtc)_2(NO)_2$, 66793-49-5; $W(Et_2dtc)_2(NO)_2$, 39872-71-4; *cis*-$Mo(Et_2dtc)_2(NO)_2^-$, 79102-45-7; ^{15}N, 14390-96-6.

(28) Coucouvanis, D. *Prog. Inorg. Chem.* **1970**, *11*, 233.
(29) Callahan, R. W.; Brown, G. M.; Meyer, T. J. *J. Am. Chem. Soc.* **1975**, *97*, 894.
(30) McCleverty, J. A.; Atherton, N. M.; Locke, J.; Wharton, E. J.; Winscome, C. J. *J. Am. Chem. Soc.* **1967**, *89*, 6082.
(31) Nicholson, R. S. *Anal. Chem.* **1966**, *38*, 1406.
(32) Carlin, R. L.; Canziani, F.; Bratton, W. K. *J. Inorg. Nucl. Chem.* **1964**, *26*, 898.
(33) Johnson, B. F. G.; Al-Obaidi, K. H.; McCleverty, J. A. *J. Chem. Soc. A* **1969**, 1668–1670.